Molecular Crystals and Liquid Crystals
Publication details, including instructions for authors and subscription information:
http://www.tandfonline.com/loi/gmcl16

Electro-convective Flows and Domain Instablilities in Nematic Liquid Crystals

L. M. Blinov [a] , A. N. Trufanov [a] , V. G. Chigrinov [a] & M. I. Barnik [a]
[a] Organic Intermediates and Dyes Institute, 103787, Moscow, U.S.S.R.
Version of record first published: 14 Oct 2011.

To cite this article: L. M. Blinov , A. N. Trufanov , V. G. Chigrinov & M. I. Barnik (1981): Electro-convective Flows and Domain Instablilities in Nematic Liquid Crystals, Molecular Crystals and Liquid Crystals, 74:1, 1-18

To link to this article: http://dx.doi.org/10.1080/00268948108073690

Mol. Cryst. Liq. Cryst., 1981, Vol. 74, pp. 1–18
0026-8941/81/7404–0001 $06.50/0

Printed in the United States of America

Electro-Convective Flows and Domain Instabilities in Nematic Liquid Crystals†

L. M. BLINOV, A. N. TRUFANOV, V. G. CHIGRINOV and M. I. BARNIK
Organic Intermediates and Dyes Institute 103787, Moscow, U.S.S.R.

(*Received July 4, 1980; in final form November 5, 1980*)

The a.c. instabilities have been investigated for homogeneously oriented layers of nematic liquid crystals (NLC) with negative dielectric anisotropy ($\epsilon_a < 0$) and for homeotropically oriented NLC layers with $\epsilon_a > 0$. It is shown that electro-convective "isotropic" flows of a liquid near the electrodes play crucial role in the formation of optical domain structures. A mechanism is discussed for the threshold destabilization of an initial director field in thin oriented NLC layers.

1 INTRODUCTION

In isotropic dielectric liquids exposed to an a.c. external field there can appear electrohydrodynamic (EHD) instabilities of the electro-convective type.[1] A good example is the well-known Sumoto effect.[2] The EHD instabilities characteristic of isotropic liquids can also occur in anisotropic ones, i.e. in liquid crystals. However, up to the recent time[3–6] the possibility of arising the electro-convective processes at alternating voltages was not taken into account and a liquid crystal was always considered as a medium having strong anisotropy of its physical properties.

Thanks to the optical anisotropy of liquid crystals the electro-convective flows destabilizing an initial molecular orientation can be observed visually and this fact makes easier their experimental investigation. We have shown earlier [3,5] that the electro-convective flows caused by an a.c. electric field give rise to the domain EHD instability in homeotropically oriented NLC layers with $\epsilon_a = \epsilon_{\parallel} - \epsilon_{\perp} > 0$. At the same time, this case is considered to be the stable one[7] in the framework of the two-dimensional theory based on the well-

† Presented at the Eighth International Liquid Crystal Conference, Kyoto, July 1980.

known Carr-Helfrich model. In thin layers of NLCs exposed to a high-frequency field domains appear in the form of Maltese crosses. The flows producing these domains in the nematic phase have also been observed in the isotropic phase using foreign particles of solid impurities, that is why this domain instability has been called the "isotropic".

It has also proposed in [3,5] that the EHD instability of homogeneously oriented layers of NLCs with $\epsilon_a < 0$ at the frequencies above the inverse of the dielectric relaxation time can be accounted for by the "isotropic" mechanism as well. At threshold this instability appears in the form of linear ("prechevron") domains (above the threshold they transform to the chevron structure[8] which is traditionally referred to the dielectric regime of the Carr-Helfrich instability.[9]) Recently Ribotta and Durand[10] have doubts about the isotropic mechanism of the domain appearance based on the different dependences of the two thresholds (for convective flows and optical domain pattern) and the sharp increase in domain threshold with increasing temperature up to the nematic-isotropic phase transition point. The authors of [10] have confirmed the existence of the "isotropic" flows of a liquid, however, refused to consider them as a main reason for director destabilization.

The purpose of this paper is a further experimental and theoretical investigation of the high-frequency regime of EHD instability in homeotropically ($\epsilon_a > 0$) and homogeneously ($\epsilon_a > 0$) oriented NLC layers in order to elucidate the geometry of flows and the reason for director destabilization. As a result, we confirm the "isotropic" mechanism.

2 EXPERIMENTAL TECHNIQUE

The experiments were carried out on pure MBBA and MBBA doped (up to ~10 weight %) with either the *p'*-cyanophenyl ester of *p*-heptylbenzoic acid (CEHBA) or 2,3-dicyano-4-pentyloxyphenyl ester of *p*-pentyloxybenzoic acid (DCEPBA). Doping allowed the control of dielectric anisotropy of the substance over the range from −2 to +2. Some experiments were carried out on either pure or doped mixture of azoxycompounds (mixture A[11]) as well as on *p*-pentyl-*p'*-cyanobiphenyl (5CB). Special measurements were performed using *p*-octyl-*p'*-cyanobiphenyl (8CB) and *p*-cyanobenzylidene-*p'*-octyloxyaniline (CBOOA) having $\epsilon_a \approx 7.5$ and both the nematic and smectic A phases. As a result 8CB has positive Leslie's coefficient α_3 over the whole nematic range.[12] CBOOA is characterized by a change in sign of α_3[13,14] with decreasing temperature from the isotropic-nematic (t_{NI}) to nematic-smectic A (t_{NA}) phase transitions.

The electrical conductivity and its anisotropy were either changed in controllable way or maintained constant ($\sigma_\parallel \sim 3 \div 5 \cdot 10^{-11}\,\mathrm{Ohm}^{-1}, \mathrm{cm}^{-1}\,\sigma_\parallel/\sigma_\perp \approx 1.5 \div 1.6$) using tetrabutyl ammonium bromide as a dopant. For these fixed

values of $\sigma_{\parallel}$ and $\sigma_{\parallel}/\sigma_{\perp}$ the domain instability in the nematic phase appeared in the form of Maltese crosses ($\epsilon_a > 0$, homeotropic orientation) or pre-chevron domains ($\epsilon_a < 0$, homogeneous orientation) over a wide frequency range of applied voltages (20 Hz–2 kHz).

EHD instabilities were studied using sandwich-type cells of thicknesses 5-105 μ. The homogeneous orientation was obtained by rubbing SnO_2-coated glass plates and homeotropic one was a result of careful mechanical and chemical refinement of SnO_2 surfaces. The instability thresholds for the nematic phase were measured using optical observation of domain appearance and solid particles motion under a polarization microscope. In addition, we could measure the optical transmission of a cell placed between crossed polaroids as a function of applied voltage. The transmission increased as a result of light diffraction by domain structures (all diffracted light was focused onto a photo-detector). The threshold of EHD instability in the isotropic phase was determined only by optical observation of solid particle motion.

To investigate the topology of the electro-convective flows in the nematic and isotropic phases we also used cells of special form which allowed the observations of EHD instability either along the normal to plates ($\parallel$ with field) or from a butt end just between plates ($\perp$ to field). The thicknesses of NLC layers, i.e. the distance between electrodes, were varied from 30 to 105 μ and the transverse size of cells corresponding to the side direction of viewing was about 1.5 mm.

The threshold voltages (U_{th}) were measured with an accuracy of $\pm 5\%$ for domain instabilities in the nematic phase and $\pm 10\%$ for onset of particles motion both in the nematic and isotropic phases.

3 RESULTS

A. Homeotropic orientation

First of all let us consider the EHD instability for homeotropically oriented NLCs with $\epsilon_a > 0$. In this case at fixed frequency and increasing amplitude of sinusoidal voltage one can notice two characteristic points, namely, the appearance of vortex flows of a liquid at a certain threshold voltage and the appearance of optical domain pattern at the second threshold.

The electroconvective flows can detected observing the motion of solid particles of foreign impurities. Let the XY plane and Z-axis of the Cartesian coordinate system coincide with the layer plane and field direction, respectively. Then the observation along Z-direction shows that above the first threshold the particles execute a circular motion in XY-plane. Observing this motion from the side direction (along the X or Y direction) one can see that the vortices occur only in narrow (of the order of one or several micrometers) layers adjacent to electrodes. The velocity of particle circulation, i.e. the velocity of

the vortex flow increases with increasing voltage. At the second critical voltage or, in other words, at the critical value of the vortex velocity a domain pattern appears which has the form of Maltese crosses. For instance, for cell thickness $L = 36$ μm and $f = 500$ Hz the pattern arises at the voltage $U_{th} = 220$ V corresponding to vortex angular velocity $v \approx 2 - 5$ revolution per second ($\epsilon_a = +0.1, t = 25°C$). The process of domain formation has a well pronounced threshold character. A microphotograph of this domain structure is given in Figure 1a. Such a pattern can be observed along Z-direction under a microscope with crossed polarizers. The Maltese crosses appear just at the same places of a cell where the vortex flows have been existing at lower voltages.

At low frequencies ($f \leqslant 100$ Hz) both the diameter of the circular traces for the particle motion and transverse dimensions of Maltese crosses are comparable with the cell thickness. With increasing frequency the distance between vortices (or between crosses) remains practically constant but their dimensions decrease. Within the limits of one Maltese cross the directions of vortex flow near opposite electrodes are opposite and such an anti-correlation can be also observed below the threshold of optical pattern appearance.

B. Homogeneous orientation

The microphotograph of the optical pattern in the form of linear pre-chevron domains at $f > f_c$ is shown in Figure 2 for a homogeneously oriented layer of NLC with $\epsilon_a > 0$. However, these domains also have as precursors the electroconvective flows in narrow layers near both electrodes. The thickness of these layers is of the same order as that for homeotropically oriented NLCs with $\epsilon_a > 0$.

We assume that the Cartesian XY-plane is the plane of a cell and the X- and Z-axes coincide with the director and field direction respectively. The domain

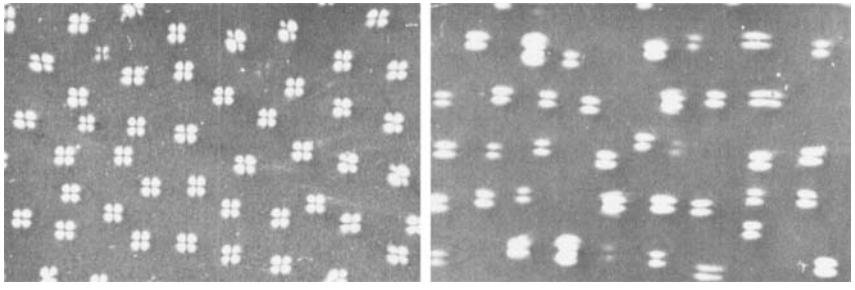

a) b)

FIGURE 1 Domain patterns for EHD instability in homeotropically (a) and homogeneously (b) oriented layers of NLCs with $\epsilon_a > 0$ (doped MBBA, $\epsilon_a = +0.05$, $\varphi_{\parallel} = 4 \cdot 10^{-11}$ Ohm^{-1}·cm^{-1}, $L = 22$ μm, $f = 100$ Hz, $t = 22°C$). Photograph size 600×400 μm.

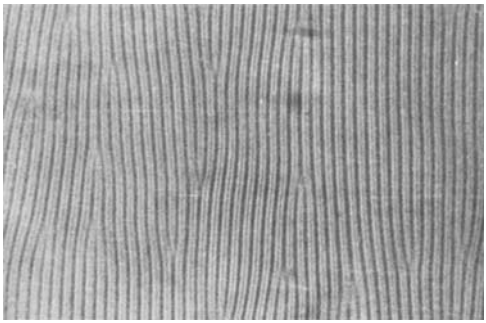

FIGURE 2 Domain pattern for EHD instability in a homogeneously oriented NLC layer with $\epsilon_a < 0$ (MBBA, $\epsilon_a = -0.55$, $\sigma_{\parallel} = 3 \cdot 10^{-11}$ Ohm$^{-1} \cdot$cm^{-1}, $L = 100$ μm, $f = 40$ Hz, $t = 22$°C). Photograph size 600 × 400 μm.

structure shown in Figure 2 is seen from the Z-direction and domain strips are oriented along Y-axis. When observing the instability from the X- or Y-directions (looking between glasses) one can see that foreign particles execute an oscillatory motion directed along the field and located again in narrow regions near electrodes. It is very difficult to elucidate exactly the geometry of their trajectories which are comparable with the size of particles. The motion of a liquid appears to be circular as big elongated particles reveal somersault-like motion. The plane of the vortices probably concides with the YZ-plane. The frequency of the oscillatory (or somersault-like) motion does not correlate with the applied field frequency but increases with increasing the field amplitude. The appearance of an optical domain pattern corresponds to some critical velocity (or frequency) of the vortices. For instance, at the applied field frequency $f = 20$ Hz the domain pattern appears when the particle oscillatory frequency reaches the value of 3–5 Hz (MBBA, $\epsilon_a = -0.55$, $L = 65$ μm, $t = 23$°C).

C. Common features of the two instabilities

Let us consider in more detail the threshold characteristics of flows and optical domains which have much in common for the two cases of interest, the homeotropic and homogeneous orientations.

a) The threshold voltage (U_{th}) of the convective instability (flows) increases with increasing frequency always according to law $U_{th}^{F} \sim f^{1/2}$ (see Figures 3, 4). The slope of curves $U_{th}^{D}(f)$ for the domain pattern depends on dielectric anisotropy ϵ_a. This dependence is in accordance with the frequency dependence of the domain period for different ϵ_a (see the insert to Figure 4).

b) At a fixed frequency the threshold for the domain pattern increases linearly with ϵ_a in the case of $\epsilon_a > 0$ (Figure 5). For $\epsilon_a < 0$ the situation is more

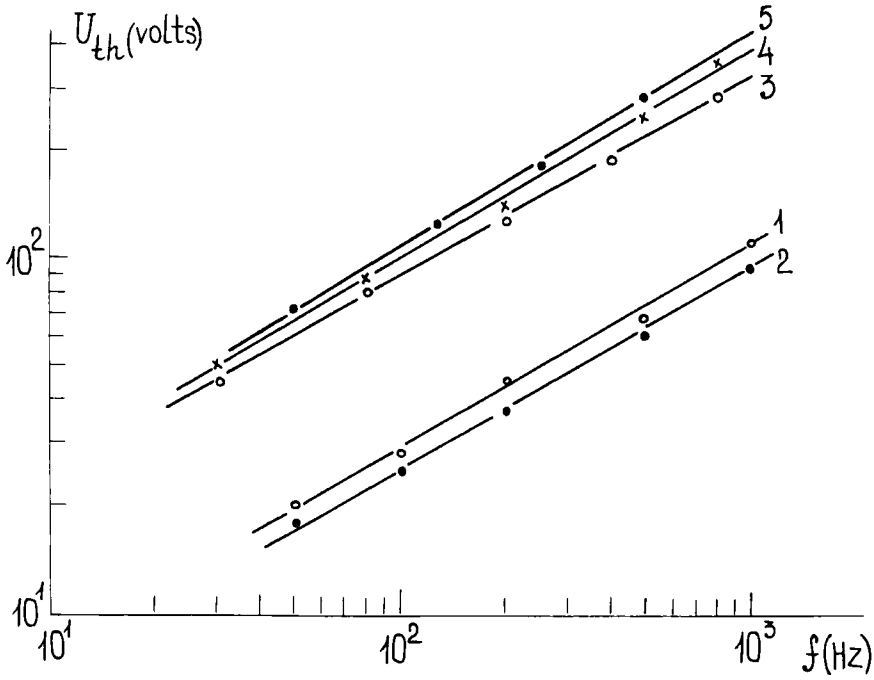

FIGURE 3 Frequency behaviour of the threshold voltages for vortex flows (1,2) and domain pattern (3–5) in homeotropically oriented NLC layer with $\epsilon_a > 0$ (doped MBBA, $\epsilon_a = +0.1$ (1,3), $\epsilon_a = +0.75$ (4), $\epsilon_a = +1.75$ (2,5); $\sigma_{\parallel} = 5 \cdot 10^{-11}$ Ohm^{-1}·cm^{-1}, $L = 36$ μm, $t = 21$°C).

complicated: the behaviour of curves $U^D_{th}(\epsilon_a)$ as well as of the period $W_{th}(\epsilon_a)$ (see the insert to Figure 5) depends on field frequency. However, the threshold curves for two cases coincide in the point where $|\epsilon_a| \sim 0$, i.e. we have the same threshold for pre-chevron domains and Maltese crosses. The threshold voltage for the convective instability (curve 1 in Figure 5) decreases slightly and symmetrically with increasing $|\epsilon_a|$ and this dependence can be accounted for by an increase in the mean value of dielectric permittivity ($\bar{\epsilon}$) of these mixtures.[3,5]

c) Both the instability branches (for flows and domains) have a field threshold, i.e. $U_{th} \sim L$. However, the slope of the threshold-thickness curves is markedly less for the flow branch, Figure 6 and less dependent on ϵ_a. The two thresholds are almost equal at small cell thicknesses and it was the case we investigated earlier.[3,5]

d) With increasing temperature both the thresholds pass through minimums near the nematic-isotropic phase transition temperature, Figures 7, 8. Such a minimum has been observed earlier[10] only for the domain threshold in homogeneously oriented layers of NLCs with $\epsilon_a > 0$. Careful measurements

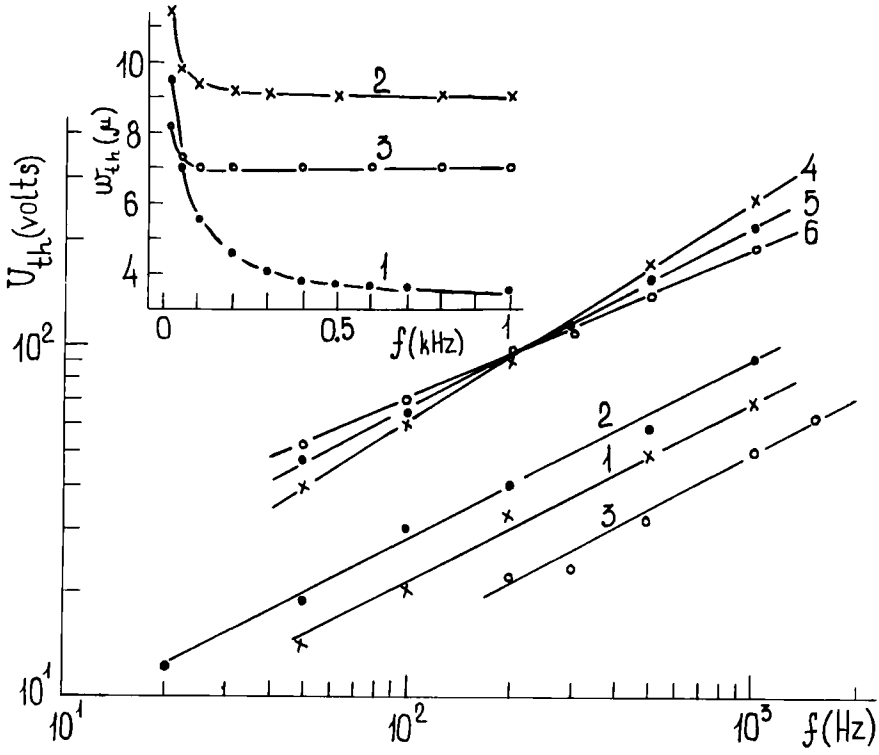

FIGURE 4 Frequency behaviour of the threshold voltages for vortex flows (1–3) and domain pattern (4–6) in a homogeneously oriented NLC layer with $\epsilon_a < 0$ (doped MBBA, $\epsilon_a = +0.05$ (1,4), $\epsilon_a = +0.55$ (2,5), $\epsilon_a = -1.25$ (3,6); $\sigma_{\parallel} = 5 \cdot 10^{-11}$ Ohm$^{-1} \cdot$cm^{-1}, $L = 36$ μm, $t = 24$°C). Insert: frequency behaviour of the period of pre-chevron domains at the threshold for $\epsilon_a = -0.05$ (1), -0.55 (2), and -1.25 (3); $L = 36$ μ.

show the existence of the minimum for the convective branch, too. Moreover, there is a correlation in the forms of "flow" and "domains" threshold curves for both the geometries under investigation, which points to the unity of physical mechanisms for flow and domain formation. Above the clearing point the domain pattern, naturally, disappears but flows can still be observed in narrow regions near electrodes. In the isotropic phase the vortices always occur in the XY-plane irrespective to the direction of their precursors in the nematic phase.

e) It can be seen from written above that flows are located near electrodes. Nothing has been said, however, about the geometry of the director distortion. To study this geometry we have carried out some experiments with special boundary conditions. First of all we found that pre-chevron domains ($\epsilon_a < 0$) are located at the angle of 45° to the directors on the limiting surfaces of an usual twist-cell. Thus, the maximum contribution to the optical pattern

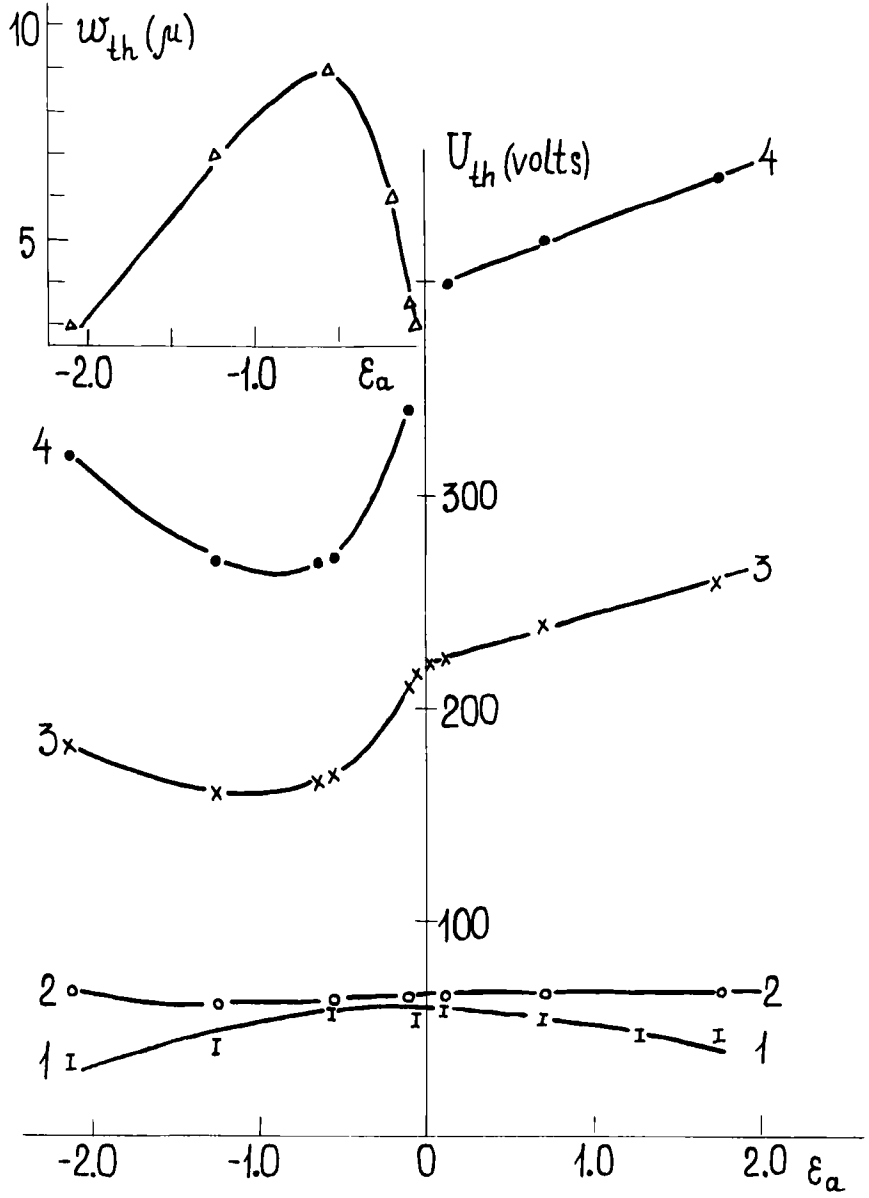

FIGURE 5 The threshold voltages for flows (1) and domain pattern (2–4) as functions of dielectric anisotropy (doped MBBA, $\sigma_{\parallel} = 5 \cdot 10^{-11}$ Ohm$^{-1} \cdot$ cm^{-1}, $f = 500$ Hz, $t = 21°C$, $L = 12$ (2), 36 (1,3) and 66 (4) μm. Insert: the period of pre-chevron domains at the threshold as a function of $\epsilon_a (L = 36\ \mu)$.

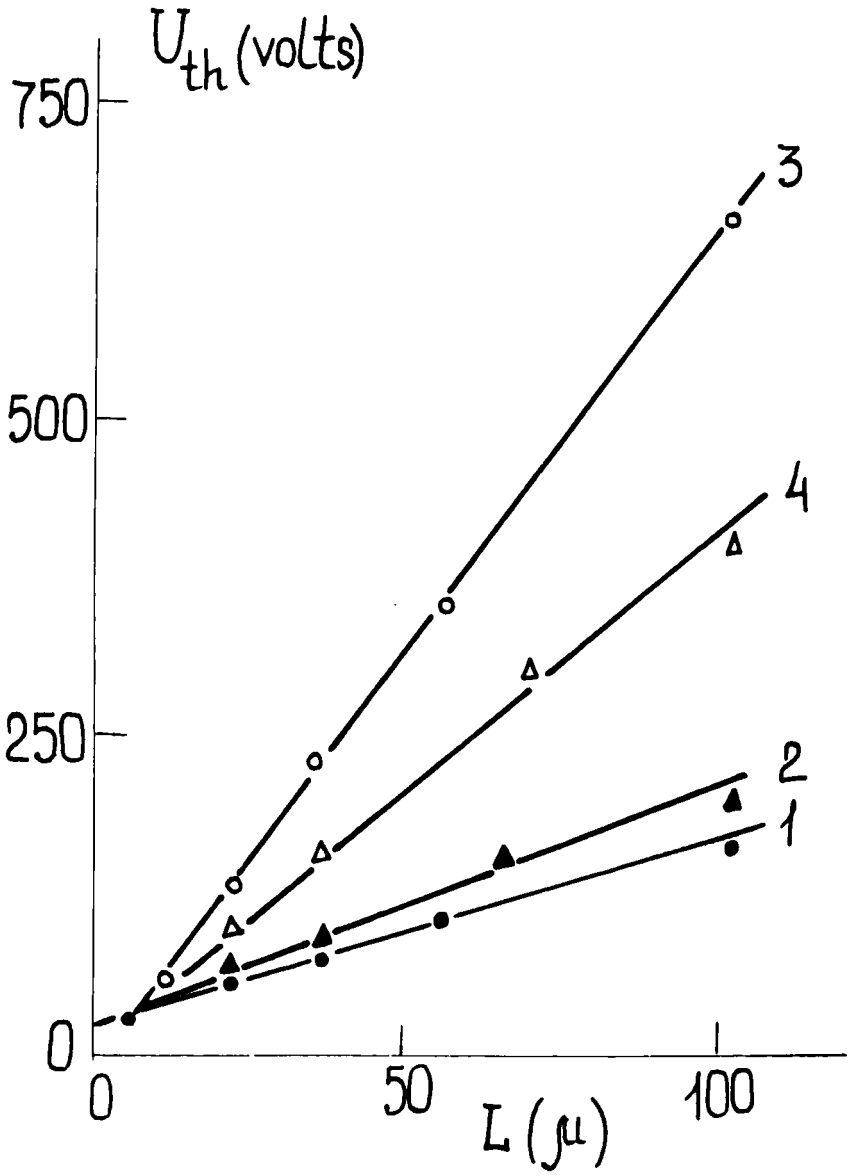

FIGURE 6 The threshold voltages for flows (1–2) and domain pattern (3–4) as functions of the thickness of an NLC layer (doped MBBA, $\epsilon_a = +0.1$ (1,3), -0.55 (2,4); $\sigma_{\parallel} = 3.8 \cdot 10^{-11}$ Ohm^{-1} $\cdot$cm^{-1}, $f = 500$ Hz, $t = 21$°C).

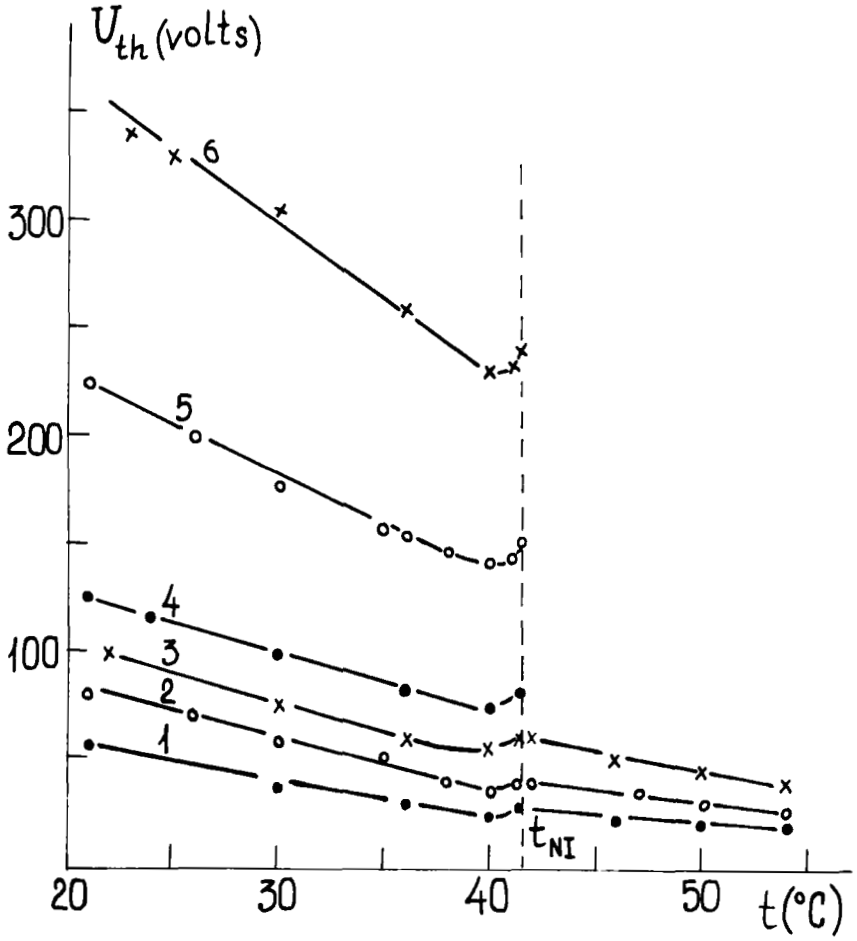

FIGURE 7 Temperature behaviour of the threshold voltages for appearance of flows (1–3) and domain pattern (4–6) in homeotropically oriented NLC layers (doped MBBA, $\epsilon_a = +0.1$, $f = 500$ Hz, $L = 22$ (1,4), 36 (2,5) and 58 (3,6) μm).

is given by the central region of a cell i.e., the distortion caused by the flows adjacent to electrodes distributes all over the cell.

We can estimate the thickness of the surface layers (h) where flows are developed using the Frederiks transition as a mean for controllable change of the molecular orientation in those layers. For example, we use NLCs with $\epsilon_a < 0$ (MBBA, $\epsilon_a = -0.05$) and make the homeotropic orientation. Then the Frederiks transition begins before the convective instability, however, at the threshold of this instability the molecules near electrodes are still perpendicular to them and flows occur in the XY-plane. With increasing voltage the process of the Frederiks reorientation is developed from the middle of a cell to

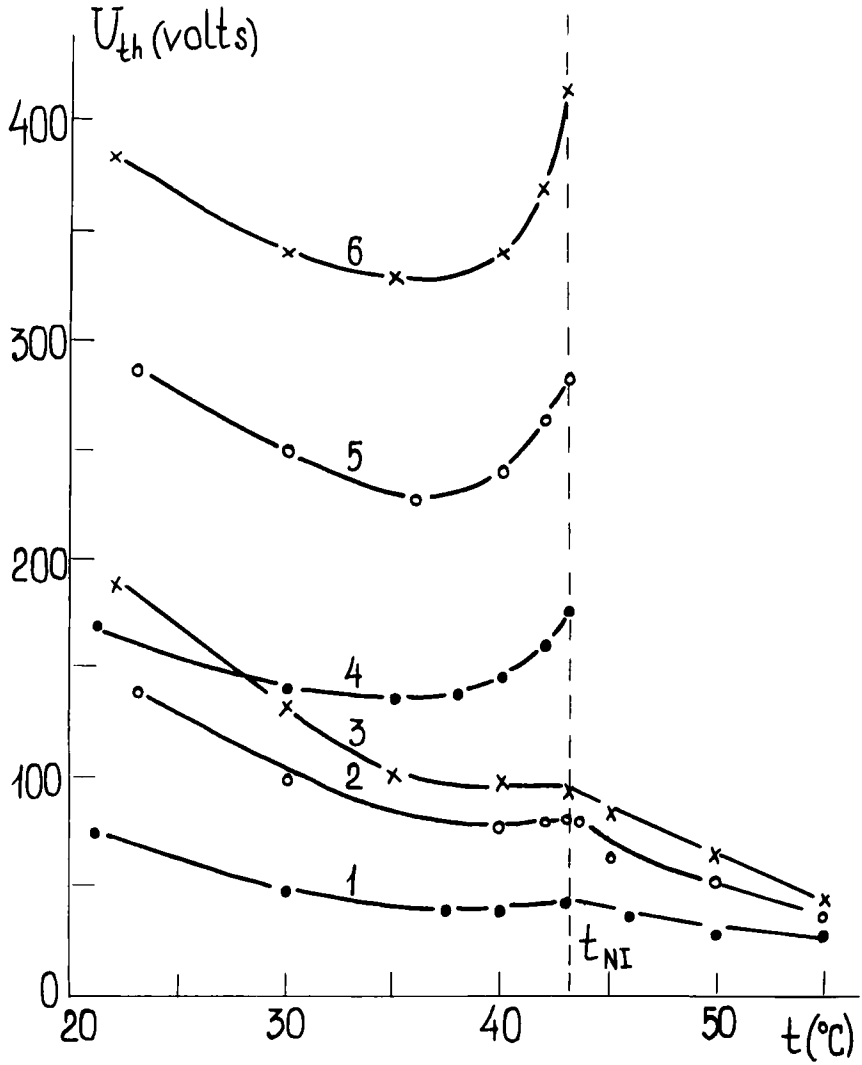

FIGURE 8 Temperature behaviour of the threshold voltages for appearance of flows (1,3) and domain patterns (4–6) in homogeneously oriented NLC layers (MBBA, $\epsilon_a = +0.55, f = 50$ Hz, $L = 36$ (1,4), 64 (2,5) and 102 (3,6) μm).

electrodes and at a certain voltage the coherence length $\xi = L/U(4\pi K_{33}/\epsilon_a)^{1/2}$ becomes comparable to h (K_{33} is the bend elastic modulus.) At this moment the direction of flows changes from XY- to YZ-plane and we can calculate h from the condition $h \approx \xi$ for the corresponding voltage.

Just in the same way we can calculate h for the case of homogeneously oriented layers of NLCs with $\epsilon_a > 0$. For instance, for doped MBBA with

$\epsilon_a = +0.05$ the Frederiks threshold voltage (U_S) is 20 V and at the frequency 40 Hz the oscillatory flows appear at 40 V for cell thickness $L = 65$ μm. At the voltage $U = 80$ V (i.e., for $\xi = L/U\,(4\pi K_{11}/\epsilon_a)^{1/2} \approx 3$ μm) the geometry of flows changes to the form characteristic of the homeotropic orientation (vortices in the XY-plane), and we conclude that $h \approx 3$ μm. In this case optical pattern appear at $U = 110$ V and it has a form of "beans" (Figure 1b) instead of Maltese crosses as a result of spoilt cylindrical symmetry near electrodes.

The experiment shows that the surface layer thickness h depends upon field frequency ($h = 3$ μ for $f = 40$ Hz, $h \approx 1.7$ μ for $f = 400$ Hz) and this result is in accordance with the model for the a.c. instability appearance in the isotropic liquid.[5]

The similar results have been obtained for all NLCs investigated: pure and doped mixture *A*, 5CB, 8CB and CBOOA.

4 DISCUSSION

Two conclusions can be derived from the analysis of experimental data.

a) Just in the same way as for isotropic liquids exposed to an a.c. electric field an electro-convective instability of threshold character occurs in liquid crystals. The instability appears in the form of vortex flows localized in narrow layers near electrodes. In the nematic phase the topology of flows depends on the initial molecular distribution near the electrodes. These facts are evident directly from experimental observations.

b) The appearance of optical domain patterns in NLCs (in the form of Maltese crosses or pre-chevron strips) is a result of destabilization of the initial molecular distribution by those (isotropic) vortex flows. This conclusion requires for some theoretical analysis which will be demonstrated below.

So, we should discuss the destabilization of the director distribution which gives rise to optical domain patterns. We adopt the existence of vortex flows as an experimental fact and, at present, we are not interested in a mechanism for flow formation.† In other words, we presuppose no positive feedback between the appearance of a hydrodynamic process and the director reorientation (such a feedback, for instance, takes place in the Carr-Helfrich instability model). So, our problem, in principle, reduces to the problem of shear-induced hydrodynamic instability for NLC director.[15] The detail calculations of the threshold shear rate for such an instability have been carried out recently

† The corresponding theory for an isotropic liquid[4-6] takes into account the field-induced space charge gradient along field direction, $dQ/dZ = -\nu E$, where ν is an electro-kinetic coefficient.[22] The principal reason for convective flows is a destabilization of this non-uniform charge distribution.

in[16,17] for various two-dimensional flow velocity profiles with account taken of stabilizing effect of external electric or magnetic field. In our case, the convective flows have special geometry but destabilize the initial director orientation in accordance with the mentioned model.[15-17] In this process an external electric field plays two parts. On one hand, being the reason for the EHD process it sets the value for velocity of a liquid and consequently plays an indirect destabilizing role. On the other hand, it directly stabilizes the director in the two geometries investigated.

Let us discuss the hydrodynamic destabilization of the director separately for the homogeneously and homeotropically oriented layers and start with the latter case which is simpler because of the cylindrical symmetry of the problem.

A. Homeotropic orientation, $\epsilon_a > 0$

Let us choose the cylindrical coordinates and assume in accordance with experiment that of three velocity component $\mathbf{V} = (V_r, V_\varphi, V_z)$ the most important is the circular one $V_\varphi(r, z), |V_\varphi| \gg |V_z|, |V_r|$. Let us assume additionally that the velocity distribution over a single vortex can be substituted by that for the rotation of thin solid cylindrical wall of radius r_0 and height h in an immobile liquid[18] (effective radius of the vortex $r_0 \gg h$ in accordance with experiment). The height of the wall h is considered to be equal to the thickness of the surface layer where flows are observed (according to,[4-6] h is an effective diffusion length where the charge gradient responsible for instability takes place). The distributions of V_φ along the Z-axis and over the cell plane are depicted in Figure 9. The analytical expression for velocity V_φ satisfying the Navier-Stokes equation can be written as follows[19]

$$V_\varphi = V_0 \sin \frac{\pi Z}{h} \exp(\pm \pi \cdot \sqrt{\bar{\eta}} \cdot (r - r_0)/h), r \gg h \qquad (1)$$

where the signs ($\pm$) refer to the V_φ values inside and outside the cylindrical wall respectively, $V_0 = V_\varphi|_{r=r_0, z=h/2}$ is a maximum velocity of wall rotation, $\eta = (\alpha_4 + \alpha_5 - \alpha_2)/\alpha_4 \gtrsim 1$ is a dimensionless combination of Leslie's coefficients.[6]

So, the velocity V_φ has two gradients, one along the normal to the layer plane ($\partial V_\varphi/\partial z$) and the other along the radius of a vortex ($\partial V_\varphi/\partial r$), and each of them, in principle, can produce the destabilization of the director field.

According to[20] the gradient $\partial V_\varphi/\partial z$ has to give rise to the deviations of the director by angle θ proportional to the gradient (without any threshold). Such deviations have not been observed in our experiments (the domain instability has a well pronounced threshold character). The estimations[19] show that angles θ are very small ($\theta \ll 1$) if all the Z-variations of velocity (ΔV_φ) occur in a thin layer h satisfying the conditions $\Delta V_\varphi \cdot h/\pi \ll K/|\alpha_2|$ (K is the effective

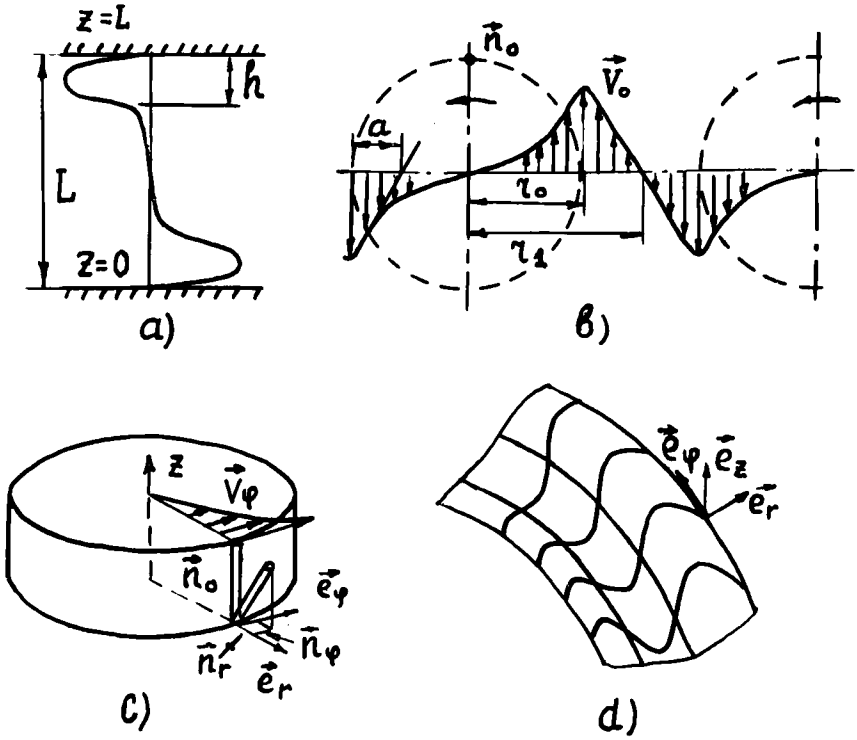

FIGURE 9 The model for the director destabilization by a vortex flow. a) the profile of the circular velocity V_φ along the Z-axis perpendicular to electrodes (L and h are the thickness of a cell and near-electrode layer, respectively). b) the profile of V_φ along the radial direction V_0 is velocity of rotation for a hypothetical wall of radius z_0, r_1 is a total radius for a vortex). c) the deviation of the director ($\mathbf{n}$) from the initial homeotropic orientation in the cylindrical coordinate system, $\mathbf{n} = (n_z, n_\varphi, n_z)$. d) the periodic alteration of the director components n_r and n_φ inside the circular domain whose axis coincides with that for the vortex.

elastic modulus). Further on we shall neglect the gradient $\partial V_\varphi/\partial Z$ and, to a first approximation, consider the destabilization of the director to result only from the gradient $\partial V_\varphi/\partial r$. According to[15] such gradients must give rise to threshold destabilization phenomena.

Having solved the equations for the director,[16] using a linear approximation, and the boundary conditions according to Figure 8a,b and taking into account the non-linear distribution of velocity from Eq. (1) one obtains the critical gradient value $(\partial V_\varphi/\partial r)_{\text{crit}}$ depending on the r-coordinate. In so doing, the director distortion are assumed to appear first of all in narrow regions h near electrodes ($h \ll r_0$) and then spread over the sample so that the optical pattern results from the all cell volume.

Two threshold modes were predicted in[15,16] for the case when the director is perpendicular to both the velocity gradient and velocity itself: the "uniform" distortion and rouleax domains. In our case, on the contrary to,[15,16] the desta-

bilizing gradient itself varies along the vortex radius, thus, the first mode will be substituted by circular domains and the second (non-uniform) should be replaced by similar circular domains with rouleax inscribed into them.

The estimations carried out in[19] show that for the "uniform" mode the threshold gradient $(\partial V_\varphi/\partial r)_{\text{crit}}$ is inversely proportional to the term $(\alpha_3 \cdot \alpha_2)^{1/2}$. Thus, the threshold should diverge at $\alpha_3 \to \theta$. We have performed such an experiment using CBOOA in the nematic phase where α_3 changes sign with varying temperature,[13,14] the sign of α_2 being constant. However, we failed to observe any peculiarity of the threshold-temperature curve in this temperature range, Figure 10. In addition, the appearance of domains and the threshold value for an electric field remain similar for two homologues of the cyanobiphenyl series, one of them (5CB) having negative and the other (8CB) positive α_3 over the whole nematic range. These results bring us to conclusion that, in our case, the "uniform" destabilization does not realize. That is why we have qualitatively analysed the other possibility ("domains inside domains") using the results of Ref. (16) with allowance made for a strong stabilizing effect of an external electric field on the director ($\epsilon_a > 0$).

Assuming the gradient

$$S = \left.\frac{\partial V\varphi}{\partial r}\right|_{r=r_0} \approx \frac{\pi\sqrt{\tilde{\eta}\, V_0}}{h}$$

to work at a characteristic length $a \sim h/\pi\sqrt{\tilde{\eta}}$, Figure 9, we search for a critical gradient S_{crit} which corresponds to a minimum value of s for all possible values of wave vector q_r of the non-uniform instability.

$$S_{\text{crit}} = \min s\,(q_r) \tag{2}$$

with the curve $S(q_r)$ specified by Eq. (5.9) (for q_x) of Ref. (16).

Based on visco-elastic coefficients for MBBA[21] and having regard to the stabilizing torque $\epsilon_a E^2$ corresponding to our experiment we have estimated the values of S_{crit} from Eq. (2) and compared them with experimental data. For instance, taking $h \approx 0.05$L, $\epsilon_a = 0.1$ and $V_{\text{th}}^D = 220$ V we get $(V_0)_{\text{crit}} \cdot L \approx 2 \div 8 \cdot 10^{-4}$ cm^2 S^{-1} for α_3 varied from -0.1 to -0.01 cP. This result qualitatively agrees with the experimental value $(V_0)_{\text{crit}} \approx 3 \cdot 10^{-2}$ cm S^{-1} for $L \approx 40$ μm. The calculation also shows that $(V_0)_{\text{crit}}$ has no peculiarity when α_3 changes its sign [$(V_0)_{\text{crit}} \cdot L \approx 9 \cdot 10^{-4}$ cm$^2 \cdot S^{-1}$ at $\alpha_3 = 0$]. The critical gradient increases markedly with increasing stabilizing action of a field at the expense of ϵ_a growth. E.g., it follows from the experiment that the variation of ϵ_a from $+0.1$ to $+0.75$ ($L = 36$ μm, $f = 200$ Hz,) results in the increase of the threshold voltage for domain formation from 120 to 130 V (Figure 3) and in the 1.5- or 2-times growth of the critical velocity of a liquid. The calculation yields the same change in the critical velocity for the same variation of ϵ_a if we assume $h \approx 0.05 - 0.07\,L$ in a accordance with experiment.

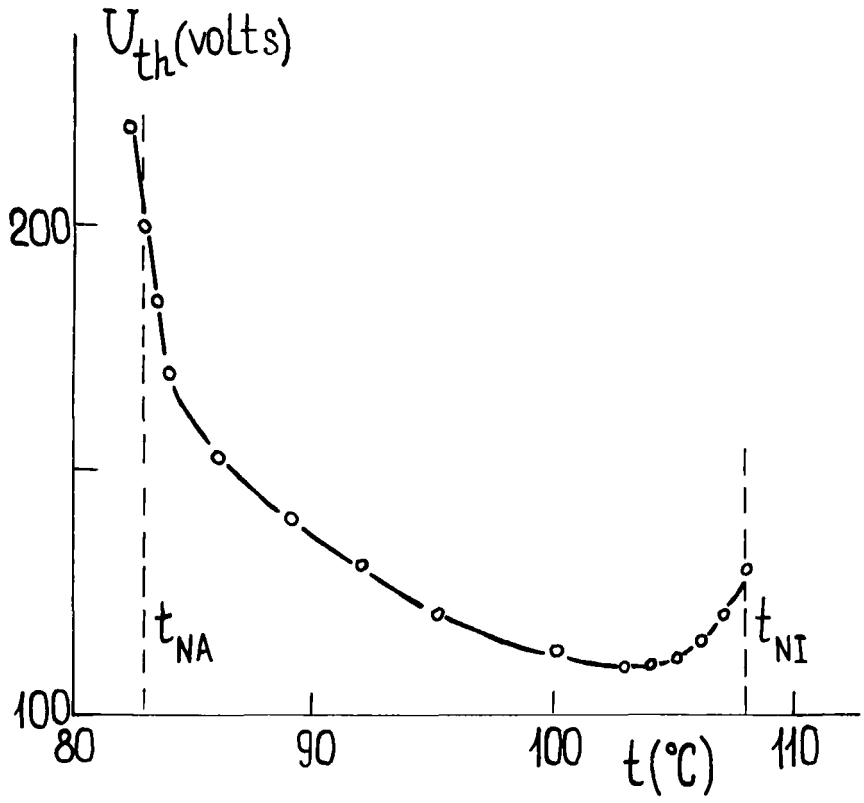

FIGURE 10 The temperature behaviour of the threshold for the domain instability in CBOOA ($L = 20$ μm, $f = 2$ kHz).

So, one can see that the suggested model is adequate to experiment. It explains practically all the observed peculiarities of the EHD instability for homeotropically oriented layers of NLCs with $\epsilon_a > 0$. First of all, the model involves two threshold processes, namely, the destabilization of a NLC as a liquid medium (the appearance of the vortex flows) and the destabilization of the director (the formation of domain patterns), and explains the difference between threshold voltages for the two processes, too. Further, it explains the frequency behaviour of the threshold for domain instability through the frequency dependence of the critical velocity of a liquid responsible for the director destabilization. The different slopes of the threshold-thickness characteristics (Figure 6) for the domain and flow instabilities is accounted for by an increase in stabilizing action of an electric field on the director (through the torque $\epsilon_a E^2$) and absense of such a direct field action on the threshold voltage for the flow formation caused by the "isotropic" mechanism. As a whole, the appearance of domain instability in homeotropically oriented NLC layers with $\epsilon_a > 0$ can be considered to be sufficiently understood.

B. Homogeneous orientation, $\epsilon_a > 0$

There are no doubts that in the case of the planar orientation the appearance of the pre-chevron domains is due also to convective vortex flows which are developed near electrodes. It follows directly from our experiments and also agrees with the results of Ref. (23). The domain pattern is completely defined by the initial director orientation and the geometry of vortices following from this orientation. Unfortunately, the flow geometry and profiles of flow velocity for this case strongly differ from those for homeotropically oriented layers. At present, we have no fairly complete data on these factors to discuss theoretically the problem of the director destabilization. If our assumption of vortex planes in near-electrodes layers having YZ-orientation is true† we would arrive in the same geometrical problem[15] for the hydrodynamic destabilization of the director. This question still waits for its theoretical solution.

The community of mechanisms for formation of the pre-chevron domains and Maltese crosses results from the following facts. Near the point $\epsilon_a = 0$ the thresholds for both the domain patterns are practically equal and the curves $V_{th}(\epsilon_a)$ don't demonstrate any divergence. There is no jump at $\epsilon_a = 0$ either in the threshold characteristic for the appearance of convective flows (Figure 5, curve 1). At fixed frequency the domain instability thresholds are very close for both the homeotropically and homogeneously oriented layers and their frequency dependencies are similar. Both the domain instabilities have a field (not voltage) threshold. Also identical are the threshold-temperature curves for homogeneously ($\epsilon_a < 0$) and homeotropically ($\epsilon_a > 0$) oriented layers. The temperature behaviour of threshold voltages for both the domain and flow instabilities is consistent with the temperature behaviour of viscosity coefficients.

5 CONCLUSION

In conclusion we would like to stress that all the EHD instabilities observed at high frequencies ($f > f_c$) in weakly conductive samples of NLCs can be explained based on the model for pure hydrodynamic destabilization of the director by convective vortex flows which are not specific for liquid crystals. In our opinion, the "dielectric" regime following from the Carr-Helfrich model[9,10] has not been observed yet. In order to detect this regime one should increase the threshold for the "isotropic" flow instability (e.g., at the expense of an increase in NLC viscosity) and lower the virtual threshold for the "dielectric" regime (for instance, thanks to an increase in the anisotropy of electrical conductivity which is possible, e.g., at frequencies where the relaxation of $\epsilon_\parallel$ occurs). In strongly conductive NLCs the lowest high-frequency

† The flows can have the form of the elongated cylinders with their axes directed along the director (the X-axis) and their lengths comparable to the cell size in this direction.

threshold corresponds to the special ("inertial") branch of the Carr-Helfrich instability in the form of "broad domains".[8] The interference of the broad and pre-chevron domains (above the threshold for the latter) in moderately conductive NLCs gives rise to the well known chevron pattern.

Acknowledgments

We are grateful to Dr. S. A. Pikin for many useful discussions stimulating the search for the theoretical explanation of the phenomena observed and Mrs. N. I. Mashirina for technical assistance during some measurements and preparation of the manuscript.

References

1. W. Pickard, *Progress in Dielectrics,* **6,** 1 (1965).
2. W. Pickard, *J. Appl. Phys.,* **32,** 1888 (1961).
3. M. I. Barnik, L. M. Blinov, M. F. Grebenkin and A. N. Trufanov, *Mol. Cryst., Liq. Cryst.,* **37,** 47 (1976).
4. S. A. Pikin, V. G. Chigrinov and V. L. Indenbom, *Mol. Cryst. Liq. Cryst.,* **37,** 313 (1976).
5. M. I. Barnik, L. M. Blinov, S. A. Pikin and A. N. Trufanov, *Zh. Eksp. Teor. Fiz.,* **72,** 756 (1977).
6. V. G. Chigrinov and S. A. Pikin, *Kristallografiya,* **23,** 333, (1978).
7. L. M. Blinov, Elektro- i magnitooptika zhidkikh kristallov, *Nauka* Moscow, 1978. (Electro- and Magneto-Optical Properties of Liquid Crystals), in Russ.
8. A. N. Trufanov, L. M. Blinov and M. I. Barnik, *Zh. Eksp. Teor. Fiz.,* **78,** 622 (1980).
9. I. Smith, Y. Galerne, S. Legerwall and F. Dubois-Violette and G. Durand, *J. Physique Colloq.,* **36,** C1-273 (1975).
10. R. Ribotta and J. Durand, *J. Physique Colloq.,* **40,** C3-334 (1979).
11. M. I. Barnik, S. V. Belyaev, M. F. Grebenkin, V. G. Rumyantsev, V. A. Seliverstov, V. A. Tsvetkov and N. M. Shtykov, *Kristallografiya,* **23,** 805 (1979).
12. K. Skarp, T. Carlsson, T. Lagerwall and B. Stebler, Third Liq. Cryst. Conf. of soc. countries, Budapest, 1979, Abstracts D-19.
13. P. Pieranski, E. Guyon, *Comm. on Phys.,* **1,** 49 (1976); M. Cohen, P. Pieranski, E. Guyon and C. D. Mitescu, *Mol. Cryst. Liq. Cryst.,* **38,** 97 (1977).
14. A. E. White, P. E. Cladis and S. Torza, *Mol. Cryst. Liq. Cryst.,* **43,** 13 (1977).
15. P. Pieranski and E. Guyon, *Phys. Rev.,* **A9,** 404 (1974).
16. P. Manneville and E. Dubois-Violette, *J. Phys. (Fr),* **37,** 285 (1976).
17. P. Manneville and E. Dubois-Violette, *J. Phys. (Fr),* **37,** 1115 (1976); P. Manneville, *J. Phys. (Fr),* **40,** 713 (1979).
18. H. Schlichting, *Grenzschicht-Theorie,* Verlag G. Braun. Karlsruhe, (1964).
19. A. N. Trufanov, M. I. Barnik, L. M. Blinov and V. G. Chigrinov, *Zh. Eksp. Teor. Fiz.* (to be published).
20. J. Wahl and F. Fisher, *Mol. Cryst. Liq. Cryst.,* **22,** 359 (1973); K. Skarp and T. Carlsson, *Mol. Cryst. Liq. Cryst.,* **49,** (Letters), 75 (1978).
21. W. H. de Jeu, *Phes. Lett.,* **69A,** 122 (1978).
22. L. D. Landau and E. M. Lifchits. Electrodinamika sploshnykh sred. Fizmatgiz, Moscow, 1959 (Electro-dynamics of Condensed Matter).
23. B. R. Jennings and H. Watanabe, *J. Appl. Phys.,* **47,** 4709 (1976).